

Quantum confinement and electroluminescence in ultrathin silicon nanowires fabricated by a maskless etching technique

This article has been downloaded from IOPscience. Please scroll down to see the full text article.

2012 Nanotechnology 23 075204

(<http://iopscience.iop.org/0957-4484/23/7/075204>)

View [the table of contents for this issue](#), or go to the [journal homepage](#) for more

Download details:

IP Address: 192.167.73.83

The article was downloaded on 10/02/2012 at 18:19

Please note that [terms and conditions apply](#).

Quantum confinement and electroluminescence in ultrathin silicon nanowires fabricated by a maskless etching technique

A Irrera¹, P Artoni^{1,2}, F Iacona¹, E F Pecora^{1,2}, G Franzò¹, M Galli³,
B Fazio⁴, S Boninelli¹ and F Priolo^{1,2}

¹ MATIS IMM-CNR, via S Sofia, 64, 95123 Catania, Italy

² Dipartimento di Fisica e Astronomia, Università di Catania, via S Sofia, 64, 95123 Catania, Italy

³ Dipartimento di Fisica 'A Volta', Università degli Studi di Pavia, via Bassi 6, 27100 Pavia, Italy

⁴ IPCF-CNR, viale F Stagno d'Alcontres 37, Faro Superiore, 98158 Messina, Italy

E-mail: francesco.priolo@ct.infn.it

Received 7 November 2011, in final form 28 December 2011

Published 25 January 2012

Online at stacks.iop.org/Nano/23/075204

Abstract

We present a novel approach for the direct synthesis of ultrathin Si nanowires (NWs) exhibiting room temperature light emission. The synthesis is based on a wet etching process assisted by a metal thin film. The thickness-dependent morphology of the metal layer produces uncovered nanometer-size regions which act as precursor sites for NW formation. The process is cheap, fast, maskless and compatible with Si technology. Very dense arrays of long (several micrometers) and small (diameter of 5–9 nm) NWs have been synthesized. An efficient room temperature luminescence, visible with the naked eye, is observed when NWs are optically excited, exhibiting a blue-shift with decreasing NW size in agreement with quantum confinement effects. A prototype device based on Si NWs has been fabricated showing a strong and stable electroluminescence at low voltages. The relevance and the perspectives of the reported results are discussed, opening the route toward novel applications of Si NWs.

(Some figures may appear in colour only in the online journal)

1. Introduction

In the last few years the scientific community has devoted an increasing interest to materials showing quantum confinement effects. Semiconductor nanowires (NWs) represent a promising system because they allow us to confine excitons in two directions. Both the electrical and optical properties are dramatically modified with respect to the bulk material, which makes them suitable candidates to become the building blocks for future electronic devices [1], photovoltaic cells [2] and sensor applications [3]. In particular, the possibility to obtain an efficient room temperature light emission from Si NWs would represent a great advancement opening the way to a wide range of new and unexpected photonic applications.

In spite of this great potential interest, light emission from Si NWs is still a scarcely reported and unexplained phenomenon. The main reason for this is probably the fact that techniques based both on the vapor–liquid–solid (VLS) mechanism and on top-down lithographic processes can only produce with difficulty wires having a suitable size to exhibit quantum confinement effects [4–6]. In addition, in the VLS mechanism the metal catalyst is usually incorporated in the NWs acting as a deep non-radiative recombination center, thus negatively altering both electronic and optical properties.

Metal-assisted wet etching processes are a known alternative method for Si NWs synthesis [7–9]. The metal catalyzes Si oxidation by H₂O₂ and then SiO₂, selectively formed where metal and Si are in contact, is etched by HF.

In metal-assisted wet etching processes the metal catalyst is usually present in the etching solution as a salt (typically AgNO_3) [7–10]. However, the use of metal salts leads to the formation of dendrites, whose subsequent removal could damage the NWs [7, 11]. Note also that NWs with mean radius lower than 30 nm have been never obtained by etching processes assisted by metal salts [11].

In this work we present a maskless, cheap, fast and compatible with Si-technology process for the direct synthesis of small Si NWs exhibiting room temperature light emission. The process is a modified metal-assisted wet etching, exploiting the replacement of the salt with a metal thin film. The thin metallic mesh injects holes into the underlying Si. In these regions Si oxidation occurs, and the presence of HF determines SiO_2 removal and the sinking of the metal into silicon, hence it produces the etching. Therefore, Si NW formation occurs in the regions which are not covered by the metal. This strategy presents two main relevant advantages: no residues due to the etching process are present and, more importantly, a better control over the Si NWs structural properties is obtained. We have indeed been able to define a precise process window where Si NWs having a diameter compatible with the occurrence of quantum confinement phenomena can be obtained. This condition has been achieved by identifying a very narrow thickness range of the Au or Ag thin films for which the layer itself is not continuous, but it is characterized by a peculiar morphology, which leaves uncovered a relevant fraction of the Si surface. Within this thickness range, the morphology of the metal layer and the etching solution determine the formation of NWs having an extremely small diameter. A strong room temperature luminescence, related to the occurrence of quantum confinement effects, is observed from Si NWs under both optical and electrical excitation, opening the way toward novel photonic applications of this material.

2. Experimental details

Si NWs have been obtained starting from p-type (B concentration of 10^{16} cm^{-3}) single crystal, (100)-oriented Si wafers. The wafers were cut into $1 \text{ cm} \times 1 \text{ cm}$ pieces, and then UV oxidized and dipped in 5% HF to obtain clean and oxide-free Si surfaces. Afterward, a thin Au layer, having a thickness of 2 or 3 nm (corresponding to 1×10^{16} and $1.6 \times 10^{16} \text{ Au atoms cm}^{-2}$, respectively), was deposited on the Si samples at room temperature by electron beam evaporation by using high purity (99.9%) gold pellets as a source. Alternatively, Ag layers 10 nm thick were deposited with the same procedure. The amount of deposited Au and Ag was verified by Rutherford backscattering spectrometry. Finally, samples were etched at room temperature in an aqueous solution of HF (5 M) and H_2O_2 (0.44 M) to form Si NWs. NWs to be employed in device fabrication have been obtained starting from highly doped p-type (B concentration of $1.5 \times 10^{20} \text{ cm}^{-3}$, corresponding to a resistivity of $8 \times 10^{-4} \Omega \text{ cm}$) single crystal, (100)-oriented Si wafers. Depending on the

doping level of the substrate, etch rate values ranging from 250 to 400 nm min^{-1} have been found.

For device fabrication, after NW formation, rectangular pieces having an area of a few mm^2 have been covered by a transparent layer (transmittance around 85% in the spectral range 480–1300 nm) of aluminum zinc oxide (AZO), having a resistivity of $0.09 \Omega \text{ cm}$ and a thickness of 1.3 μm , deposited by RF magnetron sputtering. The device has been completed by depositing a Au layer, 900 nm thick, on the backside of the Si substrate.

NW structural characterization was performed by scanning electron microscopy (SEM) and by transmission electron microscopy (TEM) techniques. SEM analyses were performed by a field emission Zeiss Supra 25 microscope. TEM analyses were performed on single NWs scratched from the substrate and collected on a copper grid by using a 200 kV JEOL 2010F microscope, equipped with a Gatan Image Filter. Micro-Raman spectra have been acquired by a HR800 spectrometer (Horiba Jobin Yvon), exciting the system with the 364 nm line of an Ar^+ laser, that allows us to avoid the spectral contribution of the substrate due to its low depth penetration in Si (about 12 nm). The power used was 4 μW to prevent heating effects. Photoluminescence (PL) measurements were performed by pumping with the 488 nm line of an Ar^+ laser. The laser beam was chopped by an acousto-optic modulator at a frequency of 55 Hz. PL signals were analyzed by a single-grating monochromator and detected by a water cooled photomultiplier tube. PL lifetime measurements were performed by monitoring the decay of the PL signal after pumping to steady state and switching off the laser beam. PL risetime measurements were performed by monitoring the increase of the PL signal up to steady state after switching on the laser beam. The overall time resolution of our system is 200 ns. Electroluminescence (EL) has been measured by biasing the device with a DC regulated power supply (ELIND HS). Light emitted from an area of $200 \mu\text{m} \times 200 \mu\text{m}$ has been collected through a $20\times$ microscope objective and then sent to a grating spectrometer (Acton SP2300) equipped with a liquid nitrogen cooled Si CCD detector (Spec 400BR, Princeton Instruments).

3. Results and discussion

3.1. Structural characterization

In the inset to figure 1(a), a SEM image of a Si surface after 3 nm Au deposition is shown. Dark regions are uncovered Si, while yellowish regions represent Au. It is clear that several nanometric uncovered Si areas, almost circular and totally embedded within Au regions are present, these are indeed the precursor sites where NWs will form upon etching. Similar structures are also observed after Ag deposition though in this case Ag, as a result of a smaller wettability, tends to ball up and therefore interconnected structures leaving nanometer-size uncovered Si regions are obtained for much thicker metal layers. Figure 1 presents a statistical analysis of the almost circular precursor sites on the basis of several SEM images taken after 10 nm Ag and 2 or 3 nm Au deposition. In

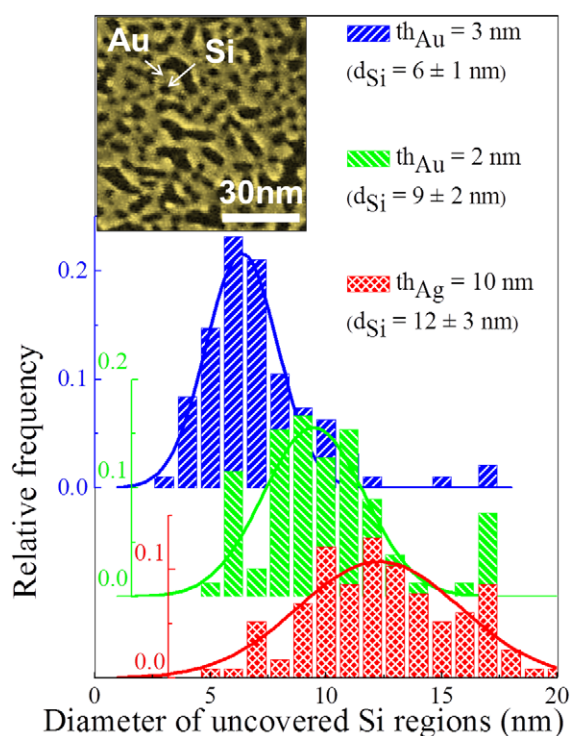


Figure 1. The inset shows a plan view SEM image of a Si surface after 3 nm Au deposition. Dark areas are uncovered Si regions while yellowish areas are Au. A statistical analysis after 3 or 2 nm Au deposition and 10 nm Ag deposition of the diameter distribution of the circular uncovered Si regions after analyzing several SEM images is reported in the figure.

all cases a nanometer-size distribution of uncovered Si regions is obtained measuring the diameter of the circle circumscribed to each precursor site, with smaller sites achieved for Au with respect to Ag and by increasing the amount of deposited Au.

Figures 2(a) and (b) report the cross section and the plan view SEM images of Si NWs obtained after the wet etching of the Au-covered Si substrates. The cross section image displays a dense and uniform distribution of NWs, having the same length (about $2.6 \mu\text{m}$, as determined by the etching conditions) and very small diameters. Particularly remarkable is the extremely high NW density ($1 \times 10^{11} \text{ cm}^{-2}$), deduced by the analysis of plan view SEM images, in which about 50% of the total surface is covered by nanowires. The density value is similar to the density of the precursor sites shown in figure 1 and is well above the typical values found for Si NWs grown by techniques based on the VLS mechanism [5, 6]. No metallic residues are detected in either image.

Raman measurements have been used to estimate the different NWs size obtained by varying the thickness of the metal layer assisting the etching process. In particular, figure 2(c) reports the Raman spectra of Si NWs synthesized by using Ag (10 nm thick) or Au (2 and 3 nm thick) metal layers; they are characterized by asymmetrically broadened peaks, red shifted with respect to the symmetric and sharper peak typical of bulk crystalline Si (shown in the same figure for comparison purposes), which is found at 520 cm^{-1} ; the position and the shape are in agreement with literature data concerning quantum confined crystalline

Si nanostructures. The Raman peaks have been fitted by using a phenomenological model developed by Richter *et al* [12] to deduce the nanocrystal size from the Raman spectrum, subsequently improved by Campbell and Fauchet [13] for strongly confined phonons and more recently applied by Piscanec *et al* to Si NWs [14]. The fit procedure gives NW diameter values of $9 \pm 2 \text{ nm}$ for the 10 nm Ag film, $7 \pm 2 \text{ nm}$ for the 2 nm thick Au film and $5 \pm 1 \text{ nm}$ for the 3 nm thick Au film. We underline here that the very large aspect ratio of these NWs can be obtained with difficulty by techniques based on the VLS mechanism. It is also remarkable that the measured NW sizes are in good agreement with the sizes of the precursor sites shown in figure 1. This is evidence that this synthesis represents a maskless method taking advantage of the thickness-dependent roughness of the metal thin film and that the deposited pattern is directly reproduced after etching.

It is noteworthy that, as a direct consequence of the peculiar characteristics of the synthesis process, based on the anisotropic etching of commercial Si substrates, NWs are monocrystalline and defect free, as verified by TEM measurements. Figure 2(d) reports a high resolution TEM image of a typical Si NW obtained by using a 2 nm thick Au film. Two features are highly remarkable: (i) a core-shell structure is clearly visible. Noticeably, Si lattice planes are visible only in the inner part of the NW, while the shell seems to be amorphous. (ii) The diameter of the crystalline core is about 5 nm, in agreement with the mean size of $7 \pm 2 \text{ nm}$ estimated by Raman measurements. Further structural details can be obtained by the analysis of the energy filtered (EFTEM) images shown in figures 2(e) and (f). The EFTEM image shown in figure 2(e) has been obtained by selecting electrons which have lost an energy of 16 eV, corresponding to the Si plasmon loss. The size of the very bright Si region fully corresponds to the crystalline region visible in panel (d), unambiguously demonstrating the presence of a crystalline Si core of about 5 nm. On the other hand, the shell appears to be much less bright than the core, suggesting a different chemical composition. A proof of the shell composition has been obtained by collecting an EFTEM image obtained by selecting electrons which have lost an energy of 24 eV, corresponding to the SiO_2 plasmon loss, shown in figure 2(f). Such an image indeed suggests that the shell is essentially composed by SiO_2 , formed due to the air exposure of the NW, and has an outer diameter of 8 nm.

3.2. Optical characterization

Si NWs synthesized by the above described technique are efficient light emitters at room temperature. Indeed, some reports about photoluminescence (PL) emission from Si NWs already exist in the literature but they are clearly not related to quantum confinement phenomena since NWs are too large and they exploit the presence of light emitting N-containing complexes [15] or the phonon-assisted low temperature recombination of photogenerated carriers [16], while only very few studies on room temperature PL from NWs whose size is reduced by poorly controllable oxidation

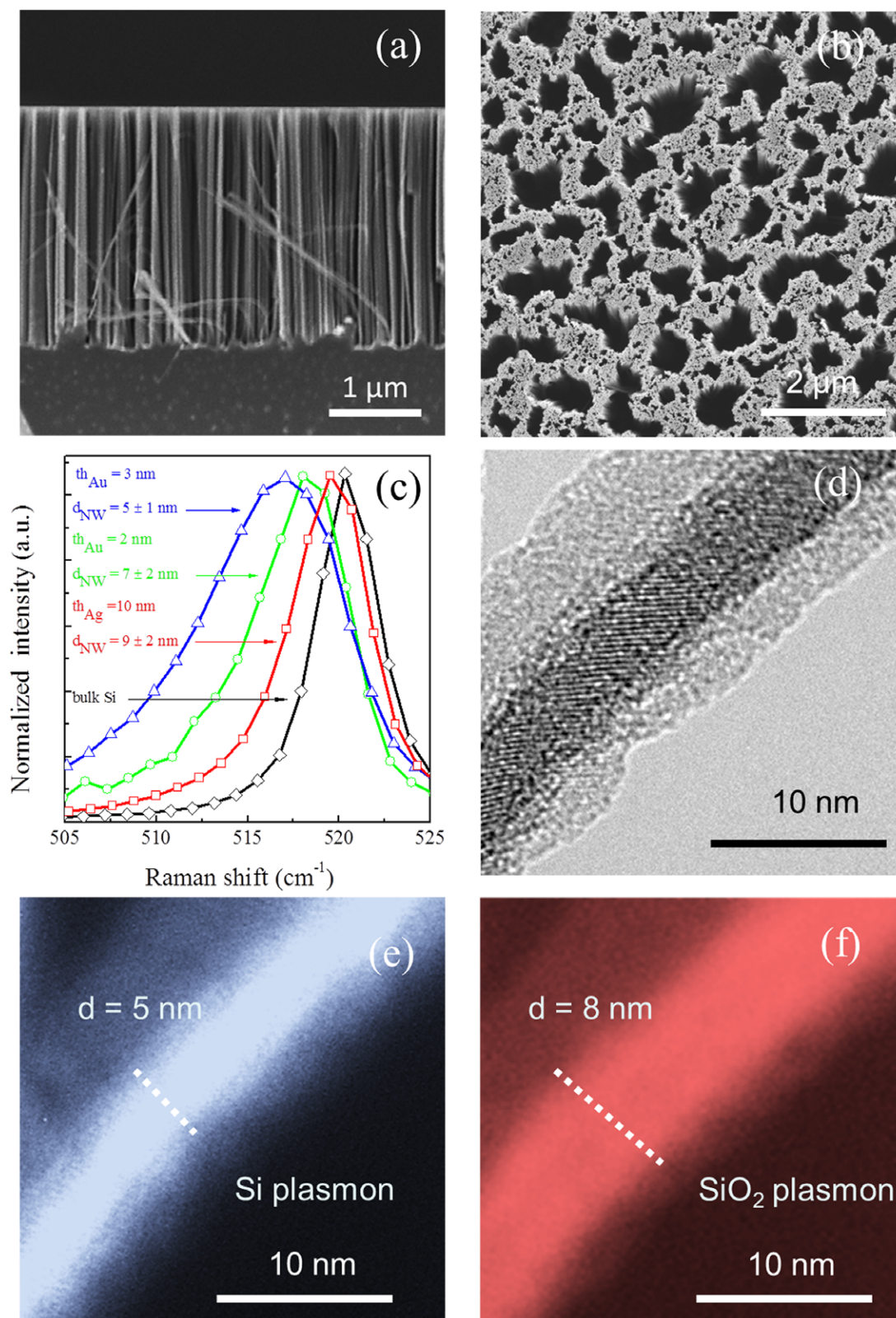


Figure 2. (a) Cross section SEM image of Si NWs obtained by the metal-assisted wet etching technique. (b) Plan view SEM image of Si NWs. (c) Raman spectra of Si NWs obtained by using Au layers having a thickness of 3 nm (blue line—triangles) and 2 nm (green line—circles) and Ag layer having 10 nm (red line—squares). For comparison, the Raman spectrum of bulk crystalline Si (black line—rhombi) is also shown. A fit to the Raman data gives NW diameter values of 5 ± 1 nm for the 3 nm thick Au film, 7 ± 2 nm for the 2 nm thick Au film and 9 ± 2 nm for the 10 nm Ag film. (d) High resolution bright field TEM image performed on a single NW. EFTEM images of the same NW shown in panel (d), obtained (e) by selecting electrons which have lost an energy of 16 eV, corresponding to the Si plasmon loss and (f) by selecting electrons which have lost an energy of 24 eV, corresponding to the SiO₂ plasmon loss.

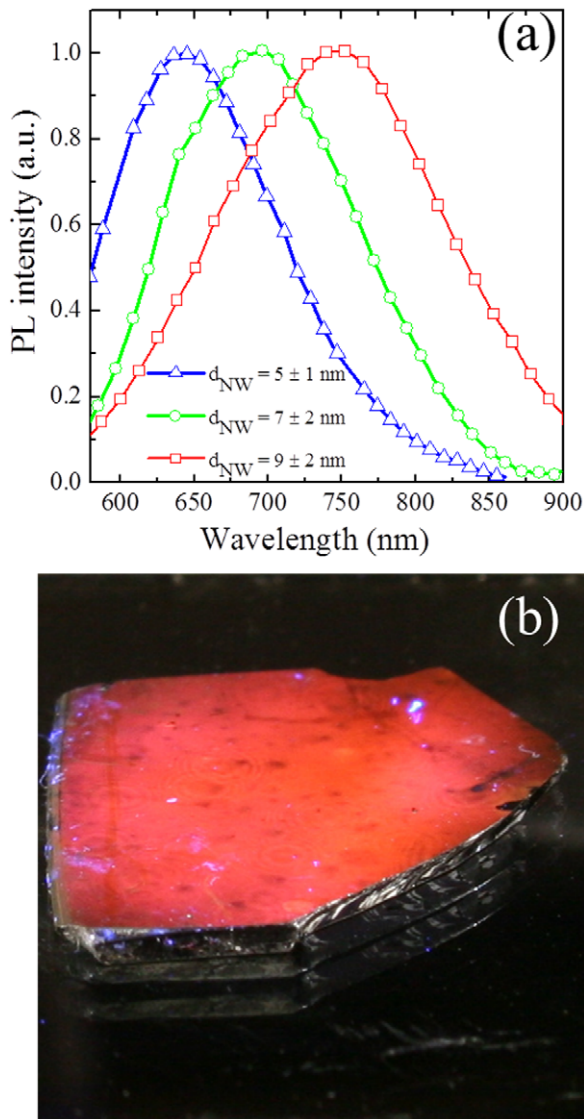


Figure 3. (a) PL spectra obtained by exciting Si NW samples having different sizes with the 488 nm line of an Ar⁺ laser at a pump power of 10 mW. (b) Photograph of a Si NW sample having an area of about 1 cm² excited by the 364 nm line of a fully defocused Ar⁺ laser beam showing a bright red PL emission clearly visible by the naked eye.

processes have been reported [17–19]. The situation is very different in the present case. Figure 3(a) reports typical PL spectra obtained by exciting with the 488 nm line of an Ar⁺ laser at a pump power of 10 mW Si NW samples having different sizes. The spectra consist of a broad band (full width at half maximum of about 150 nm) with the wavelength corresponding to the maximum of the PL emission exhibiting a shift as a function of the NW mean size. In particular, the PL peak is centered at about 750 nm for NWs having a mean diameter of 9 nm while it is clearly blueshifted at about 690 nm for NWs having a mean diameter of 7 nm and further shifted at 640 nm for a size of 5 nm. This behavior strongly suggests that quantum confinement effects are responsible for the observed light emission. Indeed emission is very bright and visible with the naked eye. Figure 3(b) displays a

photograph of the PL emission coming from a Si NW sample excited by the 364 nm line of a fully defocused Ar⁺ laser beam. A bright red light is emitted from the whole sample area (approximately 1 cm²). The external quantum efficiency of the system has been measured to be higher than 0.5%, by taking into account the spatial emission profile of the Si NWs and under the conservative assumption that the exciting laser beam is totally absorbed by the material. This value is comparable with efficiencies reported for porous Si [20] and Si nanocrystals (ncs) [21].

PL lifetime measurements were performed by monitoring the decay of the PL signal after pumping to steady state and switching off the laser beam (overall time resolution 200 ns). The lifetime of the PL signal, measured at different wavelengths after the switching off of the excitation source, is reported in figure 4(a). The lifetime has the shape of a stretched exponential ($I_{PL} = I_0 \exp(-t/\tau)^\beta$) and increases with increasing wavelength with values in the range between 15 and 40 μ s. These values are two orders of magnitude above those reported for pillars produced by e-beam lithography plus oxidation [18] demonstrating that the quality and efficiency of the present NWs is superior by orders of magnitude. The PL properties of the system have been also analyzed as a function of the pump power in the 2–50 mW range. In this range, the PL intensity increases almost linearly by increasing the pump power, while no noticeable variation of the lifetime with increasing power is detected. This behavior suggests that non-radiative processes do not play a relevant role in the luminescence properties of the system.

Relevant information about the optical properties of Si NWs can be obtained by measuring the risetime of the PL signal as a function of the pump power. Indeed these measurements allow us to calculate the excitation cross section of the system, in a fashion previously shown for Si ncs [22]. In fact, the risetime is given by:

$$\frac{1}{\tau_{on}} = \sigma\phi + \frac{1}{\tau} \quad (1)$$

σ being the excitation cross section, ϕ the pumping photon flux and τ the lifetime. By plotting the reciprocal of the risetime values at a wavelength of 690 nm as a function of the photon flux (figure 4(b)) and by a linear fit of the data we obtain a value for the excitation cross section of about 5×10^{-17} cm². Note that very similar values have been previously reported for Si ncs [22, 23]; this fact constitutes more strong evidence of the occurrence of quantum confinement effects in Si NWs.

4. Electroluminescence properties

The capability of Si NWs to emit photons if electrically excited, and therefore to constitute the active region in Si-based light emitting devices operating at room temperature, has been tested by fabricating prototype devices. The device structure is sketched in figure 5(a): p-type Si NWs have been formed by etching a Si substrate containing a B concentration of 1.5×10^{20} cm⁻³, corresponding to a resistivity of 8×10^{-4} Ω cm; length, diameter and density

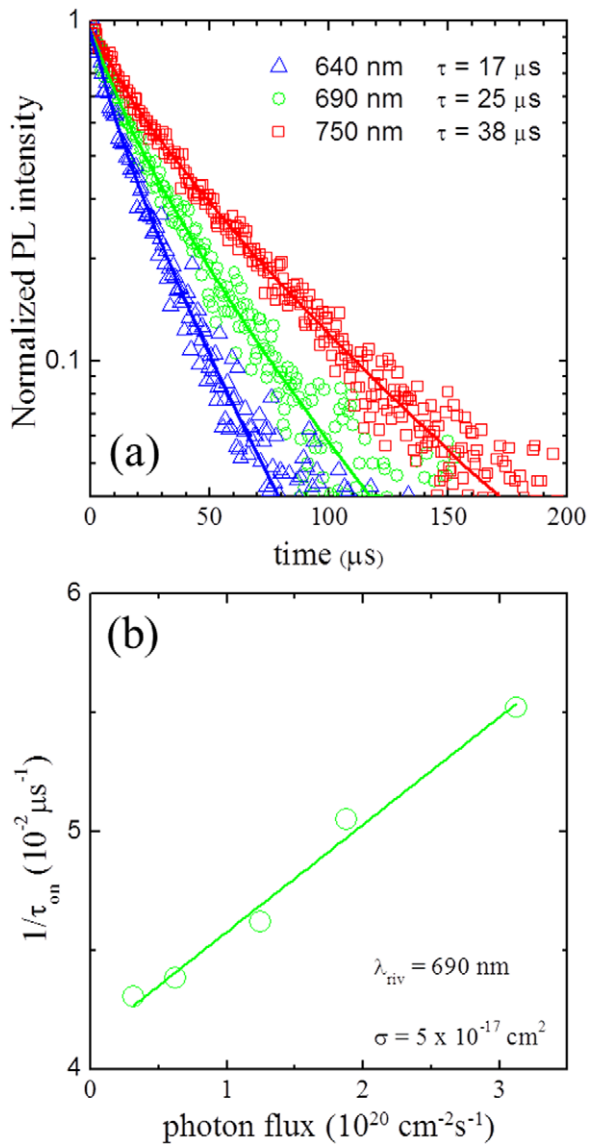


Figure 4. (a) PL lifetime of the Si NWs at different emitting wavelengths. (b) Reciprocal of the risetime as a function of the excitation photon flux. The slope of the curve gives an excitation cross section of $5 \times 10^{-17} \text{cm}^2$. The excitation wavelength was 488 nm and the detection wavelength was 690 nm.

of the NWs are very similar to those of the sample shown in figure 2(a). The electrical contacts have been realized by depositing a 900 nm thick Au layer on the back of the Si substrate and a 1300 nm thick layer of a transparent conductive oxide (AZO) on the Si NWs. AZO is a conductor n-type material, and therefore it forms a p–n junction with the underlying p-type NWs. The AZO layer allows current injection in the device without absorbing the emitted photons, being characterized by a transmittance of about 85% in the spectral range 480–1300 nm. Devices have a rectangular shape, with dimensions of the order of a few millimeter.

The EL spectra of a device forward biased at voltages between 2 and 6 V are shown in figure 5(b). They consist of a broad band, centered at about 700 nm. The shape and the

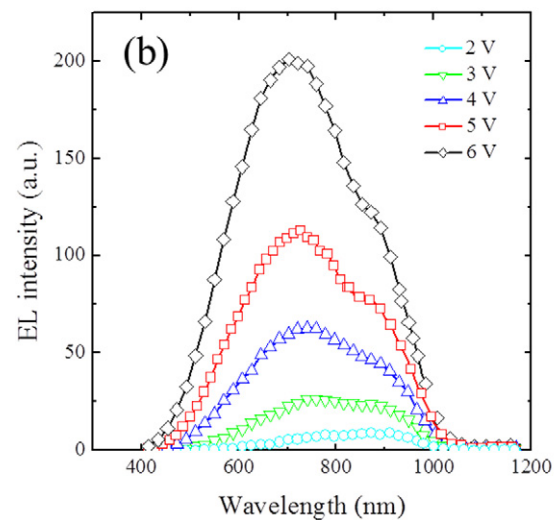
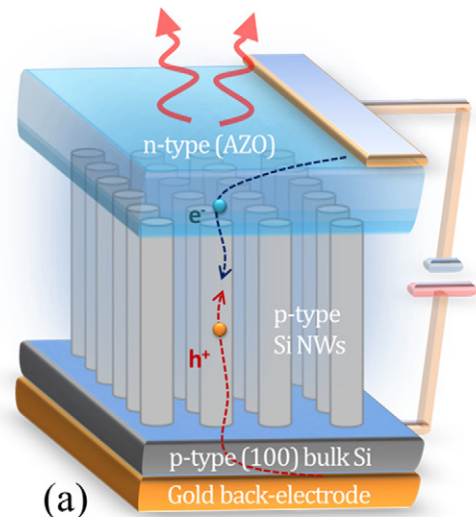


Figure 5. (a) A schematic view of the proposed device based on Si NWs. (b) The EL spectra of the device, obtained by applying a forward bias in the range 2–6 V.

position of the EL spectrum are similar to those of the PL spectra shown in figure 3(a); this similarity constitutes strong, although indirect, evidence of the fact that both mechanisms of excitation involve the same emitting centers, i.e. quantum confined Si NWs. Note that the intensity fluctuations visible in the EL spectra are due to interference phenomena induced by the presence of the AZO overlayer, while the intensity increases roughly linearly by increasing the current with operating voltages in the range 2–6 V.

5. Conclusions

In conclusion, we have demonstrated that metal-assisted etching processes can be used to produce ultrathin Si NWs exhibiting efficient RT luminescence due to quantum confinement effects. These NWs can be electrically excited and a prototype light emitting device has been demonstrated. It is noteworthy that these NWs have highly controlled and

reproducible structural properties also over very large areas, up to the wafer scale, demonstrating the potential applicability of this technique also in an industrial environment. In addition they have an electrically active dopant concentration simply determined by the doping of the etched substrate. We want to stress that changes in the concentration or in the nature of the dopant, or even the formation of p–n junctions inside the NWs, can be very simply and effectively accomplished by a proper change of the characteristics of the starting substrate. The potential advantages related to the ease of doping of Si NWs synthesized by metal-assisted etching are enormous, since, on the other hand, it is well known that the doping of NWs grown by techniques based on the VLS mechanism presents important problems, both for *in situ* [24] and *ex situ* [25] approaches, such as incomplete dopant activation [26], dopant surface segregation [26, 27] or even Si NW structural damage in the case of ion implantation [28]. It is also remarkable that there is no metal inclusion inside the NWs, which is one of the main factors which makes application in optical and electrical devices of NWs grown by metal-catalyzed VLS techniques difficult. Metal particles are indeed trapped at the bottom of the etched regions. Since the whole process is performed at room temperature, diffusion inside the wires is negligible and metal atoms can be effectively removed at the end by an appropriate selective etching.

Finally, it becomes important to compare performances and perspectives of Si NWs with those of Si ncs, which have been generally recognized as the most promising Si-based materials for applications in light sources. While Si NWs show strong similarities to Si ncs from several points of view, they have in fact much stronger potentials. Si NWs have the great advantage over Si ncs of being a continuous 1D Si system. Indeed, it is well known that tunneling phenomena are the main conduction mechanism in Si ncs embedded in SiO₂ [29]. This determines high operating voltages, which could probably prevent any practical device application of Si ncs; furthermore, oxide breakdown phenomena constitute the main failure mechanism for devices based on Si ncs. In contrast, Si NWs can be fabricated in very dense arrays, are very good conductors and we have demonstrated light emitting devices operating at low voltages (2 V). These aspects open the route toward the use of Si NWs as the most promising Si light emitting source.

Acknowledgments

We wish to thank C Spinella and C Bongiorno (CNR-IMM) for useful discussions. C Percolla, S Tati and G Lupò are acknowledged for expert technical assistance.

References

- [1] Duan X F, Huang Y, Cui Y, Wang J F and Lieber C M 2001 *Nature* **409** 66
- [2] Tian B, Zheng X, Kempa T J, Fang Y, Yu N, Yu G, Huang J and Lieber C M 2007 *Nature* **449** 885
- [3] Zhou X T, Hu J Q, Li C P, Ma D D D, Lee C S and Lee S T 2003 *Chem. Phys. Lett.* **369** 220
- [4] Wagner R S and Ellis W C 1964 *Appl. Phys. Lett.* **4** 89
- [5] Kim B J, Tersoff J, Kodambaka S, Reuter M C, Stach E A and Ross F M 2008 *Science* **322** 1070
- [6] Schmidt V, Senz S and Gösele U 2005 *Nano Lett.* **5** 931
- [7] Peng K Q, Wu Y, Fang H, Zhong X Y, Xu Y and Zhu J 2005 *Angew. Chem. Int. Edn* **44** 2737
- [8] Huang Z P, Shimizu T, Senz S, Zhang Z, Geyer N and Gösele U 2010 *J. Phys. Chem. C* **114** 10683
- [9] Peng K, Xu Y, Wu Y, Yan Y, Lee S T and Zhu J 2005 *Small* **1** 1062
- [10] Lin L, Guo S, Sun X, Feng J and Wang Y 2010 *Nanoscale Res. Lett.* **5** 1822
- [11] Peng K Q, Yan Y J, Gao S P and Zhu J 2003 *Adv. Funct. Mater.* **13** 127
- [12] Richter H, Wang Z P and Ley L 1981 *Solid State Commun.* **39** 625
- [13] Campbell I H and Fauchet P M 1986 *Solid State Commun.* **58** 739
- [14] Piscanec S, Cantoro M, Ferrari A C, Zapien J A, Lifshitz Y, Lee S T, Hofmann S and Robertson J 2003 *Phys. Rev.* **68** 241312
- [15] Shao M, Cheng L, Zhang M, Ma D D D, Zapien J A, Lee S and Zhang X 2009 *Appl. Phys. Lett.* **95** 143110
- [16] Demichel O, Calvo V, Pauc N, Besson A, Noè P, Oehler F, Gentile P and Magnea N 2009 *Nano Lett.* **9** 2575
- [17] Guichard A R, Barsic D N, Sharma S, Kamins T I and Brongersma M L 2006 *Nano Lett.* **6** 2140
- [18] Walavalkar S S, Hofmann C E, Homyk A P, Henry M D, Atwater H A and Scherer A 2010 *Nano Lett.* **10** 4423
- [19] Valenta J, Bruhn B and Linnros J 2011 *Nano Lett.* **11** 3003
- [20] Cullis A G, Canham L T and Calcott P D J 1997 *J. Appl. Phys.* **82** 909
- [21] Dal Negro L, Yi J H, Michel J, Kimerling L C, Chang T-W F, Sukhovatkin V and Sargent E H 2006 *Appl. Phys. Lett.* **88** 233109
- [22] Priolo F, Franzò G, Pacifici D, Vinciguerra V, Iacona F and Irrera A 2001 *J. Appl. Phys.* **89** 264
- [23] Kovalev D, Diener J, Heckler H, Polisski G, Künzner N and Koch F 2000 *Phys. Rev. B* **61** 4485
- [24] Schmid H, Björk M T, Knoch J, Karg S, Riel H and Riess W 2009 *Nano Lett.* **9** 173
- [25] Colli A, Fasoli A, Ronning C, Pisana S, Piscanec S and Ferrari A C 2008 *Nano Lett.* **8** 2188
- [26] Koren E, Berkovitch N and Rosenwaks Y 2010 *Nano Lett.* **10** 1163
- [27] Tutuc E, Appenzeller J, Reuter M C and Guha S 2006 *Nano Lett.* **6** 2070
- [28] Pecora E F, Irrera A, Boninelli S, Romano L, Spinella C and Priolo F 2011 *Appl. Phys. A* **102** 13
- [29] Franzò G, Irrera A, Moreira E C, Miritello M, Iacona F, Sanfilippo D, Di Stefano G, Fallica P G and Priolo F 2002 *Appl. Phys. A* **74** 1